AD

USAAVLABS TECHNICAL REPORT 68-54

FEASIBILITY STUDY OF A HYBRID VIBRATION ISOLATION SYSTEM

By

David Alan Bies

August 1968

U. S. ARMY AVIATION MATERIEL LABORATORIES
FORT EUSTIS, VIRGINIA

CONTRACT DAAJ02-67-C-0082

BOLT BERANEK AND NEWMAN INC.
VAN NUYS, CALIFORNIA

52

Disclaimers

The findings in this report are not to be construed as an official Department of the Army position unless so designated by other authorized documents.

When Government drawings, specifications, or other data are used for any purpose other than in connection with a definitely related Government procurement operation, the United States Government thereby incurs no responsibility nor any obligation whatsoever; and the fact that the Government may have formulated, furnished, or any way supplied the said drawings, specifications, or other data is not to be regarded by implication or otherwise as in any manner licensing the holder or any othe person or corporation, or conveying any rights or permission, to manufacture, use, or sell any patented invention that may in any way be related thereto.

Disposition Instructions

Destroy this report when no longer needed. Do not return it to originator.

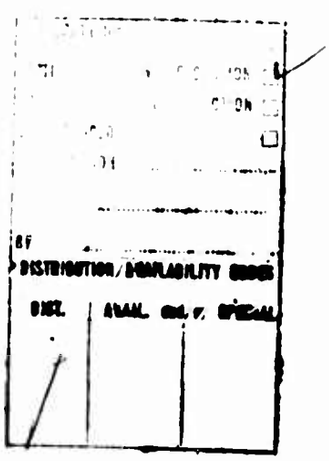

DEPARTMENT OF THE ARMY
U. S. ARMY AVIATION MATERIEL LABORATORIES
FORT EUSTIS, VIRGINIA 23604

This report has been reviewed by the U. S. Army Aviation Materiel Laboratories and is considered to be technically sound. The report is published for the exchange of information and the stimulation of ideas.

Task 1F125901A14608
Contract DAAJ02-67-C-0082
USAAVLABS Technical Report 68-54
August 1968

FEASIBILITY STUDY OF A HYBRID VIBRATION ISOLATION SYSTEM

Final Report

Bolt Beranek and Newman Inc. Report 1620

By

David Alan Bies

Prepared by

Bolt Beranek and Newman Inc.
Van Nuys, California

for

U. S. ARMY AVIATION MATERIEL LABORATORIES
FORT EUSTIS, VIRGINIA

SUMMARY

The fluctuating lift of a helicopter rotor gives rise to undesirable vibration over a broad frequency range which in some cases may extend to as low as 3 Hz. Vibration isolation over this frequency range is very difficult to achieve with either a purely passive or an active vibration isolation system. A passive system will work well at high frequencies, but it will always have a low frequency resonance where excitation will be amplified rather than reduced. An active system may work well at low frequencies, but it will have trouble meeting the frequency response requirements at high frequencies.

As part of its overall program to improve Army aviation through research, the U. S. Army Aviation Materiel Laboratories, Fort Eustis, Virginia, has sponsored the work reported here, in which the feasibility of combining the desirable properties of a passive vibration isolation system with an active vibration isolation system has been investigated. Such a system would control the undesirable resonant response of the passive system near its resonance through a feedback control loop involving a sensor and an active element. The proposed system, referred to in this report as a hybrid vibration isolation system, would operate actively at low frequencies and passively at high frequencies.

The introduction of the active element can drastically change the characteristics of a given system. Very high vibration isolation may be achieved at any particular frequency or range of frequencies. However, the requirements for ideal response at all frequencies of the hybrid system are difficult to achieve. The requirements would not be difficult if it were possible to control phase and amplitude response of a circuit independently. Since the proper phase and amplitude response of a circuit are difficult to achieve simultaneously, the feasibility of the isolation system depends upon the ability to make satisfactory engineering compromises in the design. Some, but by no means all, of those which seem reasonable and offer promise have been investigated.

TABLE OF CONTENTS

LIST OF ILLUSTRATIONS

LIST OF ILLUSTRATIONS - Continued

LIST OF TABLES

LIST OF SYMBOLS

a	acceleration
C	capacitance
C_a	accelerometer internal capacitance
E_a	accelerometer output voltage
E_{in}	input voltage
E_{out}	output voltage
f	frequency
g	acceleration of gravity
$Im()$	imaginary part of ()
i	$\sqrt{-1}$
K	complex ratio x/y
K_1	complex ratio x/z
L	inductance
M	isolated mass
M_p	platform mass
M_T	$= M + M_p$
m	$= M + M_p\ (1 + K_1)$
n	summation index
R	mechanical resistance, circuit resistance
R_a	accelerometer internal resistance
R_c	$= 2M_T\ \omega_r$ critical damping
$Re()$	real part of ()
R_m	$= R(1 + K_1)$
R_1, R_2	circuit resistances

LIST OF SYMBOLS - Continued

S	mechanical stiffness
S_m	$= S(1 + K_1)$
t	time
w	displacement of vibrating mass relative to platform
x	displacement of platform relative to isolated mass
X, Y	variables defined by Equation 12
y	displacement of platform relative to earth
z	displacement of isolated mass relative to earth
z_o	displacement of vibrating mass relative to earth
z'	initial displacement of isolated mass
α	amplitude decay constant, proportionality constant
β	resonant frequency of hybrid isolation system
γ	$= -\alpha \pm i\beta$ complex exponent
θ	phase lag due to the signal conditioning circuit
Φ	phase lag due to the valve and cylinder
Ψ	phase lag due to the accelerometer
ω	angular frequency $2\pi f$
ω_R	resonant frequency of passive system
$\dot{}$	dot over a variable indicates differentiation with time
exp( )	exponential function whose argument is ( )

INTRODUCTION

Many sources of vibration are present in helicopters. One of the primary sources is the fluctuating lift of the rotor which may give rise to vibrations as low as the fundamental frequency of the rotor. Thus, there is in some helicopters a need for vibration isolation over a broad frequency range beginning as low as 3 Hz. On the other hand, an isolation system which might isolate the fuselage or part of it from the fluctuating forces of the rotor, for example, would have to be stiff below 0.5 Hz for adequate control of the helicopter. These requirements are very difficult to meet with a purely passive vibration isolation system. In addition, passive systems always have a troublesome resonance frequency at which vibration is amplified.

The U. S. Army Aviation Materiel Laboratories, Fort Eustis, Virginia, has sponsored this investigation of the feasibility of combining an active and passive system to gain the advantages of both. The report shows that an active system may be used to control the resonant response of a passive system while preserving the isolation achieved at high frequencies. Isolation over a broad frequency range may be obtained by this means with only a small amplification of response at low frequencies.

DISCUSSION

The procedures and results of this investigation are presented in the following sections. In the section entitled General Outline of Approach, the problem and proposed method of solution are presented. Some of the practical difficulties involved in obtaining a solution are also presented. In the following section entitled Hybrid Vibration Isolation Model, the model is described and analyzed. The analysis in this section serves the purpose of providing direction for the subsequent experimental work. The results of experiments with the model are presented in the section entitled Experimental Investigation. In the section entitled Some Requirements for Implementation, attention is given to estimates of weight size and cost for the construction of a prototype. Consideration is also given in this section to fail-safe provisions.

GENERAL OUTLINE OF APPROACH

A passive isolation system will give isolation at frequencies above the square root of two times the frequency of undamped resonance, but below this frequency such a system will always amplify the excitation. The extent to which excitation is amplified at resonance depends upon the mechanical damping of the system. On the other hand, the isolation achieved is also dependent upon the system damping in such a way that isolation is always sacrificed when reduction in resonant response is obtained through damping.

It is difficult to construct a purely active system that will give vibration isolation over a broad frequency spectrum because of the difficulty of achieving high-frequency response with any nonresonant mechanical system. This report investigates the feasibility of combining an active system with a passive system in such a way that the active system will be required to operate only in a narrow frequency range about the natural resonance frequency of the passive system. Such a system will be called a hybrid vibration isolation system.

In principle, one would measure acceleration or velocity at some point on a combined passive and active system, process the signal appropriately, and feed it back to actuate an active element. The response of the active element would be such as to prevent resonant response of the isolation system. For any particular configuration of active element and response sensor, the requirements

for ideal response of the system on the signal conditioning circuit can be determined. Satisfactory engineering compromises must then be sought to approach ideal response.

An ideal isolation system would meet the following requirements. It would be stiff below some low frequency, and it would be quite soft above that frequency. A small resonant amplification of response might be acceptable if the isolation at higher frequencies were appreciably greater than would be achieved with a well-damped, purely passive system of comparable resonant response. The hybrid system proposed here could be made to act like an ideal isolation system if the active element in the system could be made to operate in a relatively narrow frequency range with the appropriate amplitude and phase. Correct phase is very important. Investigation to be described later has shown that a principal difficulty with the hybrid system is that it is very difficult to shut the active system off at low frequencies (in order to achieve a stiff system down to zero frequency) without shifting the phase in such a way as to amplify the motion.

HYBRID VIBRATION ISOLATION MODEL

As part of a program to investigate the feasibility of constructing a hybrid vibration isolation system, a model was constructed on which various ideas could be tested. The model was constructed of commercially available parts and was designed to achieve vibration isolation over the frequency range from 3 to 100 Hz. Sufficient instrumentation was incorporated to determine response over this frequency range.

Physical Description of the Apparatus

A photograph of the apparatus is shown in Figure 1a, while a pictorial representation of the apparatus is shown in Figure 1b. A block diagram of the mechanical and electrical circuitry is presented in Figure 2. As shown in Figure 1, the test vibration source consists of a hydraulic cylinder anchored to a 1700-pound inertia block shown supported at the top of the test stand. A nominal 20-pound block is shown attached to the vibration source piston. The purpose of the latter block is to provide a nominal ballast weight to smooth the response of the test shaker. The control for the test shaker is separate from, and is quite similar to, that employed for the active element of the hybrid vibration isolation system. A common hydraulic power supply was used for both the test shaker and the active element.

The mechanical arrangement for the hybrid vibration isolation system is as follows (see Figure 1). A dashpot is connected in mechanical parallel with a spring to the upper side of a plate labeled "platform" in the figure. The piston of the active element is attached in turn to the lower side of the platform. The control valve for the active element is mounted on the test stand frame (see Figure 1a) and is connected to the active element by means of flexible hoses. The active element is capable of a peak-to-peak displacement of 3.5 inches with a maximum static force output of 6000 pounds. A small box arrangement is attached to the end of the hydraulic cylinder. The latter box forms a mount for accelerometers and an attachment point for the load. The magnitudes of the various components are given in Table V, in the appendix.

The isolation system was provided with three accelerometers, two of which are shown explicitly in Figure 1b. The accelerometers and their locations are as follows. A Bruel and Kjaer accelerometer type 4332 was mounted on the ballast weight to provide a means for monitoring the excitation vibration level. A second Bruel and Kjaer accelerometer type 4334 was mounted in the attachment box at the bottom of the active element cylinder next to an Endevco accelerometer type 2219E. The former accelerometer was used as part of the feedback circuit, while the latter was used to monitor acceleration levels at the point of attachment to the load. The calibration of both accelerometers used for monitoring acceleration levels at the input and output of the system is traceable to the National Bureau of Standards. Calibration of the feedback accelerometer was not necessary.

The output voltages of the two monitoring accelerometers were read sequentially at each test frequency with a General Radio Sound and Vibration Analyzer type 1564A. The latter was calibrated at 100 Hz to read as a voltmeter in decibels re 100 millivolts by comparison with a calibrated Bruel and Kjaer vacuum tube voltmeter. The calibration of the Bruel and Kjaer voltmeter is also traceable to the National Bureau of Standards.

A block diagram of the active element feedback circuit is shown in Figure 2. The diagram shows that the system uses two feedback circuits. The inner loop consists of a position measurement accomplished with a linear voltage differential transformer (LVDT) which is fed back to a summer in the control circuit, while the outer loop consists of an acceleration measurement processed and fed

back to the same summer. The sum of the two signals is used to control the valve, which in turn activates the cylinder. The block diagram also shows that the steady-state position of the active element is controllable through a third (position) input to the summer.

The signal conditioning circuit used in the outer loop is shown in detail in Figure 3. It consists of a very low pass filter and an inverter of unity gain. Gain control in the feedback circuit was accomplished at the summer input and the General Radio Sound and Vibration Analyzer. The signal conditioning circuit was designed to give a 6-dB-per-octave roll-off above a break frequency of $1/2\pi$ Hz.

Analytical Description of the Mechanical System

A schematic representation of the hybrid vibration isolation system is shown in Figure 4. The latter will serve to define the various displacement variables. All of the variables have been taken as positive in the upward direction in the diagram. The variables y, z, and z_o are absolute displacements relative to the earth, while the variables w and x are relative displacements. The quantity which will be of principal importance will be the ratio $|z/z_o|$, since this quantity represents the degree of isolation achieved by the system.

In Figure 5, the hybrid vibration isolation system is represented by an equivalent electrical circuit. In this case, velocities of the various elements are shown by time derivatives of the various displacements. In the analog, currents are equivalent to velocities, while voltages are equivalent to forces. Figures 4 and 5 will be used interchangeably depending upon the ease of presentation afforded by one or the other.

Details of the analysis of the mechanical system shown in Figures 4 and 5 are given in the appendix. A summary of the analysis follows. Define two complex quantities K and K_1 which are functions of frequency only as follows:

$$K = x/y \qquad (1)$$

and

$$K_1 = x/z \quad . \qquad (2)$$

These quantities are related by

$$1 + K_1 = (1 - K)^{-1} \quad . \tag{3}$$

Reference should now be made to either Figure 4 or Figure 5. From Equation 1, if K approaches unity, then the variables x and y or $\dot{x}$ and $\dot{y}$ tend to be equal. In this case, either figure shows that the variable z tends to zero. The latter fact is expressed by Equations 2 and 3 taken together. Thus, for best isolation, K_1 should be very large and real.

A general solution for the hybrid vibration isolation system driven sinusoidally is obtained in the appendix. The solution is

$$z = \frac{(i\omega R + S)z_o}{-m\omega^2 + iR_m\omega + S_m} + z' \exp(-\alpha + i\beta)t \tag{4}$$

where

$$\left.\begin{aligned} m &= M + M_p(1 + K_1) \quad , \\ R_m &= R(1 + K_1) \quad , \\ \text{and} \quad S_m &= S(1 + K_1) \quad . \end{aligned}\right\} \tag{5}$$

The expressions for α and β are quite complicated for the general case with K_1 complex, but for the special case where K_1 is very large so that

$$\left.\begin{aligned} M &\ll M_p\left|1 + K_1\right| \quad , \\ \text{then} \quad \alpha &= \frac{R}{2M_p} \\ \text{and} \quad \beta &= \sqrt{\frac{S}{M_p} - \alpha^2} \quad . \end{aligned}\right\} \tag{6}$$

The first term on the right in Equation 4 describes the steady-state response, while the second term on the right describes the transient response.

Assuming that the system is stable, the steady-state response may be determined from Equation 4 by letting the second term go to zero. The response function $\left|z/z_o\right|$

may be calculated from the first term on the right of Equation 4. Besides the general solution given in the appendix, two special cases are of interest.

Suppose that the magnitude of K_1 is allowed to become zero. The system then reduces to a purely passive system. Equation 4 reduces to the following well-known expression:

$$\left|\frac{z}{z_o}\right|_{passive} = \sqrt{\frac{1 + 4\left(\frac{R}{R_c}\right)^2\left(\frac{\omega}{\omega_R}\right)^2}{\left[1 - \left(\frac{\omega}{\omega_R}\right)^2\right]^2 + 4\left(\frac{R}{R_c}\right)^2\left(\frac{\omega}{\omega_R}\right)^2}} \qquad (7)$$

where critical damping $R_c = 2 M_T \omega_R$,

$$M_T = M + M_p \quad ,$$

and $$\omega_R^2 = \frac{S}{M_T} \quad . \qquad (8)$$

A second special case of interest occurs when the real part of K_1 is allowed to become indefinitely large but the imaginary part remains bounded and small by comparison. This is the case of an ideal active isolation system. In this case, Equation 4 reduces to the following expression:

$$\left|\frac{z}{z_o}\right|_{active} = \frac{\left|z/z_o\right|_{passive}}{|K_1|} \qquad (9)$$

where now M = 0 in Equations 8. The isolation in the ideal case is independent of the isolated mass. Equation 9 shows that the ideal hybrid vibration isolation system is capable of arbitrarily small transmissibility since the response $\left|z/z_o\right|_{passive}$ is bounded, while the large quantity K_1 is unbounded.

Analytical Description of the Feedback Circuit

In this section an expression for the complex quantity K_1 will be developed. It will be shown that the real part of K_1 cannot become indefinitely large while the imaginary

part remains bounded and that the quantity K_1 allowed by system stability requirements is limited. Referring to Figure 2, the system block diagram, the procedure used will be to develop expressions for the response of individual items in the circuit starting with the Bruel and Kjaer accelerometer and proceeding around the outer feedback circuit back to the cylinder. The discussion will begin with the accelerometer.

The Bruel and Kjaer accelerometer type 4334 is essentially a crystal loaded with a small weight. It senses acceleration as a force across the crystal which induces a bound charge on its surface. Thus, the crystal produces a charge proportional to acceleration and is essentially a charge generator which looks into a parallel circuit consisting of its own internal resistance and capacitance and the detector impedance. A General Radio Sound and Vibration Analyzer was used as a detector whose input impedance is sufficiently high as to be negligible at frequencies as low as 2.5 Hz compared to the accelerometer internal impedance in parallel with it. Analysis of the simple circuit postulated here gives the following expression for the output voltage-acceleration relationship:

$$E_a \alpha\ iR_a\omega \frac{1 - iR_a\omega C_a}{1 + (R_a\omega C_a)^2} a \quad . \tag{10}$$

Experimental investigation of the voltage-acceleration relation showed that the voltage leads the acceleration by 45 degrees at 2 Hz. From this observation, using Equation 10, it is determined that

$$R_a C_a = 1/4\pi \text{ Hz} \quad . \tag{11}$$

According to the block diagram of Figure 2, the detected accelerometer voltage passes through a signal conditioning circuit. The latter circuit is shown in detail in Figure 3. Straightforward circuit analysis gives the following relationship between the input and output voltages:

$$E_{out} = \frac{R_2}{R_1} \frac{1 - iR_2C\omega}{1 + (R_2C\omega)^2} E_{in} \quad . \tag{12}$$

The quantities R_2 and C correspond to 1 megohm and 1 microfarad, respectively, in the circuit. R_1 corresponds to

the adjustable 60 kilo-ohm input resistance. With this choice of R_2 and C, the break frequency for the circuit is

$$1/2\pi \text{ Hz} \quad . \tag{13}$$

According to the block diagram of Figure 2, the output voltage from the signal conditioning circuit enters the summer. The summing amplifier accomplishes a single inversion and drives the valve. The response of the valve and cylinder as a unit will be considered as follows. The valve consists of various parts which contribute inertia and resistance. In terms of an equivalent electrical circuit, any one part might look like a series inductance and resistance with the output measured across the resistance, provided that the inductance is quite large compared to the resistance. Thus, any one part would be represented by an equation such as the following:

$$E_{out} \frac{R}{R + iL\omega} E_{in} \quad . \tag{14}$$

The various stages of the valve, the connecting tubing, and the cylinder might be represented by a series of terms such as that of Equation 14:

$$E_{out} = E_{in} \prod_n \frac{1 - i(2\pi L/R)_n f}{1 + (2\pi L/R)_n{}^2 f^2} \quad . \tag{15}$$

The number of terms and the values of the constants are determined empirically by fitting Equation 15 to measured response data. In Equation 15, E_{in} is taken as the input voltage while E_{out} is taken as the resulting displacement of the piston in the cylinder of the active element. It is found experimentally that a good fit to the measured response of the active element is given by the following equation:

$$x \alpha \left[\frac{1 - i(f/5\sqrt{3})}{1 + (f/5\sqrt{3})^2}\right]^3 E_{in} \quad . \tag{16}$$

These results may be combined to obtain an expression for the quantity K_1 defined by Equation 2. To accomplish this task, Equations 10 through 13 are combined with Equation 16 and the relationship between acceleration and displacement,

$$a = -x\omega^2 \quad . \tag{17}$$

The result of the indicated operation is

$$K_1 \alpha \frac{f^3 \exp - i(\pi/2 + 3\Phi + \theta + \psi)}{\sqrt{[1 + (f/5\sqrt{3})^2]^3 [1 + (2\pi f)^2][1 + (f/2)^2]}} \qquad (18)$$

where $\Phi = \tan^{-1} (f/5\sqrt{3})$,

$\theta = \tan^{-1} (2\pi f)$,

and $\psi = \tan^{-1} (f/2)$.

The function K_1 is determined to within an arbitrary constant by Equation 18, since the total system gain in the feedback circuit has not been specified. In practice, the system gain was determined by increasing the gain until the system was on the verge of instability but was still stable. The function K_1 has been plotted in Figure 6. The magnitude of K_1 is expressed arbitrarily in decibels relative to its value taken at 10 Hz. From measured transmissibility with an input acceleration level of -15 dB re 1 g rms at 6 Hz where K_1 is real, the magnitude of K_1 corresponding to zero decibels on the scale is found to be 3.48. This value will be useful in calculating response at other frequencies.

The effective impedance of the active element is a quantity of interest. Reference to Figure 4 or 5 and use of Equation 2 show that it may be written as follows:

$$\text{active element impedance} = \frac{i\omega M \dot{z}}{\dot{x}} = \frac{i\omega M}{K_1} \quad . \qquad (19)$$

Use of Equation 19 allows the construction of Table I.

In Figure 7, the phase of the parameter K_1 is plotted and compared with the various effective impedances shown in Table I. The estimate of the total system phase lag includes phase shift due to the accelerometer, signal conditioning circuit, active element control valve, and cylinder response.

TABLE I. EFFECTIVE IMPEDANCE OF THE ACTIVE ELEMENT

K_1 Magnitude	Phase in Degrees	Impedance
Positive real	0, -360	Mass reactance, or mass
Positive imaginary	-270	Resistance or dashpot
Negative real	-180	Stiffness reactance or spring
Negative imaginary	-90, -450	Negative resistance or generator

The estimate is based on measured and calculated response of the various elements as discussed earlier. From Figure 7, it is seen that the active element looks like a mass reactance at 6 Hz. Reference to Figure 5 then shows that the active element behaves like a very small inductance in parallel with the isolated mass inductance. In this case the active element acts like a short circuit, tending, as it should, to isolate the load.

Figure 7 shows that at approximately 2 Hz, the active element behaves like a resistance or dashpot. Reference to either Figure 4 or Figure 5 then shows that isolation will still be obtained, provided that the resistance is not large.

At 17 Hz, Figure 7 shows that the active element behaves like a negative resistance or a generator. In this case, the isolation of the isolated mass will be degraded, resulting in possible system instability. It is important to roll off the response of the active element sufficiently so that at this frequency the passive isolation may control the system response.

EXPERIMENTAL INVESTIGATION

Sinusoidal Excitation

In preliminary tests, the hybrid vibration isolation system was run as an active and a passive system. In the passive mode, the active element behaved simply as a rigid coupling (refer to Figure 1) between the platform and the isolated

mass. The results of these tests are shown in Figure 8, where it is seen that the resonant peak of the passive system is eliminated by the active element. The measurement of the resonant peak of the passive system was of incidental value in estimating the effective resistance of the dashpot. It is of interest to note that testing in the passive mode in the frequency range of resonance was restricted to very low levels, much lower than were permissible in the active mode, because of excessive displacement amplitude which threatened destruction of the spring.

The vibration isolation provided by the system for 0-, 20-, and 40-pound loads was investigated, with the results shown in Figures 9, 10, and 11. A range of excitation levels from -20 to 0 dB re 1 g rms was used in these tests. In the case of zero load, the highest levels tested were limited by the mechanical stability of the model. In the case of the 20- and 40-pound loads, the highest levels investigated (see, for example, Table II and Figures 10 and 11) were limited by the capability of the test shaker. This problem was particularly acute at low frequencies where large excursions of the piston were required.

The data in Figures 9, 10, and 11 clearly indicate that the system is nonlinear; the apparent isolation improves in the frequency range below 11 Hz, but appears to greatly degrade in the frequency range above 11 Hz as the excitation acceleration is decreased. Above 11 Hz, the isolation is due principally to the passive system. In this range, the apparent degradation in isolation is due to the residual vibration of the active system, which is high due to a common hydraulic power supply for both the active element and the test shaker. The connecting hoses unfortunately served as fairly efficient mechanical vibration links between the test shaker and the active system. Thus, in this frequency range the acceleration levels of the isolated mass remained essentially constant independent of the excitation acceleration up to the highest excitation acceleration levels tested. They were apparently controlled by vibration transmission through the hydraulic hoses rather than by vibration through the isolation system.

In the frequency range below 11 Hz, the isolation is due to the active element. The apparent degradation in isolation with increasing excitation level is apparently due to nonlinear response of the valve and cylinder at high flow rates. Thus, as long as the excursions of the piston

of the active element are not large, the system performs as expected; but at high levels of excitation, large excursions are required, in which case large flow rates result in nonlinear response. The effect is to increase the lag of the cylinder. Figure 10 shows that the isolation achieved in the frequency range between 5 and 10 Hz is extremely sensitive to level of excitation; this is interpreted here as reflecting sensitivity to extreme phase shift.

Included in Figure 10 is a curve indicating the expected response calculated using the data in the appendix and in Figure 6. As explained earlier, the magnitude of K_1 was determined from the measured isolation at 6 Hz. Thus, the theoretical curve has been fitted to the data at 6 Hz. The predicted response at 17 Hz agrees fairly well with the measured response for high excitation. The divergence at 2.5 Hz is probably due to inadequacy in the estimate of K_1 at this frequency.

In Figure 12, some of the results shown in the previous figures are replotted for comparison to show the effect of changing the load. The theory given in the appendix indicates, and the data show, that the isolation is insensitive to the load imposed by the isolated mass.

Figure 13 shows a comparison of the hybrid vibration isolation system and a passive system with a resonance at approximately 2 Hz. Response curves are given for various values of damping ratio referenced to critical damping for the system (see Equation 7). It is apparent that the data shown fit the curve determined for a damping ratio of 0.5. Comparison of Figures 8 and 13 shows that the introduction of the active element has drastically altered the behavior of the passive system; however, amplification at some low frequency has been retained.

As pointed out earlier, the hydraulic system is quite nonlinear (see Figures 10 and 11); therefore, the experimental result shown in Figure 13 can be expected to change with higher input levels. In Figure 14, the measured vibration isolation observed with 1 g rms excitation or the highest excitation vibration obtainable with the test shaker is shown. The excitation levels are given in Table II.

Included in Figure 14 are the data obtained with the hybrid vibration isolation system in the passive mode. For comparison, the calculated response of a passive system with

TABLE II. HIGHEST EXCITATION LEVELS OBTAINABLE WITH A 20-POUND LOAD

Frequency in Hz	Acceleration Level in decibels re 1 g rms	Acceleration Level in g rms
3	-9	0.36
4	-7	0.45
5	-6	0.50
6	-4	0.63
7	-5	0.56
8	-5	0.56
10	-3	0.71
15	0	1.00
15 to 100	0 and greater	

a damping ratio of 0.034 (see Equation 7) is included in the figure. The figure shows that the hybrid vibration isolation system has essentially preserved the isolation obtainable with a lightly damped passive system except for slight losses at 7 and 8 Hz, but it has completely eliminated the large resonant peak of the passive system. A stiff system with a fairly rapid roll-off has been achieved with the hybrid vibration isolation system. The same requirement cannot be met with any passive system. It is also doubtful whether an active system could provide the broad upper frequency range of isolation of which the hybrid vibration isolation system is capable, since in this range the hybrid vibration isolation system makes use of a purely passive system.

Repeated Shock Excitation

Test of the response of the hybrid vibration isolation system to repeated shock was provided by driving the test shaker with square wave and sawtooth wave voltage inputs to the control. The test shaker responded with a square wave or sawtooth wave velocity, thus giving rise to either acceleration of alternately positive and

negative spikes or square wave acceleration. Two repetition frequencies, 5 and 10 Hz, were used for these tests. The results for broadband frequency response are contained in Table III.

During each test, the excitation acceleration and the isolated mass acceleration were Fourier analyzed using a General Radio Sound and Vibration Analyzer 1/10 octave filter. The results of these operations are shown in Table IV. The data were used to compute the isolation at each harmonic frequency. The data shown in the last column of Table IV show isolation in terms of acceleration amplitudes, but since the results are for the Fourier components of acceleration, the same data hold for velocity or displacement amplitudes. The data show that no excessive deflections were experienced. The isolation achieved is generally in line with the results of sinusoidal testing with the exception that for sawtooth wave excitation, the fundamental frequency at 10 Hz was reduced by only 3 decibels. The latter result may be due to nonlinearity of the hydraulic system at high excitation levels.

Impact Shock Excitation

The effectiveness of the hybrid vibration isolation system as an impact shock isolation system was investigated as follows. The isolation system (see Figure 1) was disconnected from the test vibration source ballast weight and reconnected to a steel rod approximately 2 feet long. The rod was fitted with the vibration isolation system hanging vertically through a clearance hole in one of the horizontal cross members at the top of the test stand. The rod was terminated in a large nut. The system was lifted up to a prescribed mark on the steel rod and allowed to drop. The fall was abruptly terminated by contact between the nut on the end of the rod and the previously mentioned cross member at the top of the test stand.

Tests were run successively with and without the active feedback system functioning. The system was dropped successively from heights of 4-5/8 inches and 18-3/4 inches, giving simulated landing velocities of 5 feet/second and 10 feet/second. The tests were conducted with the 20-pound load as the mass to be isolated.

A repeat of three drops with the system in a passive mode and a simulated landing velocity of 5 feet/second gave peak accelerations on the load of 14 dB above 1 g or 5 g acceleration. Three repeat tests with the system in an active mode gave peak acceleration levels of the

TABLE III. BROADBAND ISOLATION OBSERVED WITH A 20-POUND LOAD FOR REPEATED SHOCK EXCITATION

Type Excitation	Repetition Frequency in Hz	Excitation Acceleration $\ddot{z}_o$ in decibels re 1 g rms	Isolated Mass Acceleration $\ddot{z}$ in decibels re 1 g rms	Isolation $-20 \log \lvert \ddot{z}/\ddot{z}_o \rvert$ in decibels
Square Wave	5	-5	-15	10
	10	0	-7	7
Sawtooth Wave	5	-9	-14	5
	10	-5	-13	8

TABLE IV. EXPERIMENTAL RESULTS WITH A 20-POUND ISOLATED MASS FOR REPEATED SHOCK EXCITATION

Square Wave Excitation Repetition Frequency in Hz	1/10 Octave Analysis			
	Center Frequency in Hz	Excitation Acceleration $\ddot{z}_o$ in decibels re 1 g rms	Isolated Mass Acceleration $\ddot{z}$ in decibels re 1 g rms	Isolation $-20 \log \lvert \ddot{z}/\ddot{z}_o \rvert$ in decibels
5	5	-12	-16.5	4.5
	10	-33.5	-51.5 to -41.5	18 to 8
	15	-10	-20.5	10.5
	20	-33	-41.5 to -40.5	8.5 to 7.5
	25	-10.5	-27.5	17
	35	-11	-37.5	26.5
	45	-13.5	-35.5	22
	55	-16.5	-39.5	23
	65	-19	-37.5	18.5
	75	-21	-37.5	16.5
	85	-19	-36.5	17.5
	95	-19	-45.5	26.5
10				
	10	- 4	- 7	3
	31	- 3.5	-33.5	30
	51	- 8.5	-34.5	26
	73	-11.5	-30	18.5
	93	-13	-48.5	35.5

TABLE IV - Continued

Sawtooth Wave Excitation Repetition Frequency in Hz	1/10 Octave Analysis			
	Center Frequency in Hz	Excitation Acceleration $\ddot{z}_o$ in decibels re 1 g rms	Isolated Mass Acceleration $\ddot{z}$ in decibels re 1 g rms	Isolation $-20 \log \lvert \ddot{z}/\ddot{z}_o \rvert$ in decibels
5	5	-11	-14	3
	10	-30	-33	3
	15	-20	-41	21
	20	-32	-42	10
	25	-27	-36	9
	35	-30	-38	8
	45	-33	-44	11
10	10	- 6	-13	7
	20	-26	-33	7
	30	-15	-35	20
	50	-24	-36	12

load of 12 dB above 1 g or 4 g acceleration. The hybrid vibration isolation system thus reduced the impact acceleration level by about 20 percent. It was also noticed that the active system tended to inhibit bouncing after impact though no qualitative measurements of this effect were attempted.

When the system was dropped from an 18-3/4-inch height, the attachment of the spring to the platform broke. It has subsequently been determined that the spring-platform connection, a weld, was not optimum and that methods of attachment are available by which this fault may be eliminated. The system was in the active mode, and a peak acceleration level of 20 dB re 1 g or 10 g was recorded during this test. Testing was terminated because of the attachment failure.

SOME REQUIREMENTS FOR IMPLEMENTATION

Weight, Power and Cost Estimates

The development of the hybrid vibration isolation system is in a very preliminary stage, and the possible mode of incorporation of the system in a vehicle is not defined. Thus, estimates of weight, power, and cost will be made in terms of the model investigated in this report. Such estimates may serve as a starting point for extension to other systems which might be considered.

The model considered in this report uses a 2-inch-diameter piston and a 2000-psi hydraulic power supply. For a 1 g rms acceleration level at 3 Hz, a volume flow of approximately 58 cubic inches per second is required. If all of the pressure head is dissipated across the valve and cylinder, the implied power is 17.5 hp. If half of the pressure drop is across the cylinder, then a 3000-pound force will be generated by the active element under these circumstances. The model required less than 1/30 of the available force, leading to the conclusion that the power dissipated in the valve and active element was less than 0.6 hp. However, the power requirement to maintain the pressure head without some means of recovery would remain 17.5 hp.

The weight of the hybrid vibration isolation model and valve was of the order of 20 pounds. For a 20-hp system, the weight of the hydraulic power supply might be of the order of 200 pounds including the pump and associated hardware. The system might be contained within a space of 3 cubic feet. The estimated cost to construct a

prototype isolation system similar to the one discussed in this report, but with an improved cylinder and valve, would be of the order of $3700. This system would be able to effectively isolate up to a 600-pound mass at 3 Hz for an excitation acceleration of 1 g rms. The full available force of the active system probably could not be used because of degradation of system performance with the implied large flows.

Consideration of Fail-Safe Provisions

In the event of failure of the isolation system, two possibilities are presented: first, when complete shutdown of the isolation system is tolerable though not desirable, and second, when complete shutdown of the isolation system is intolerable. If the second possibility is the case, then the system must be redundant with provision for rapid switching incorporated in its structure. If the first possibility is the case, then the fail-safe provision may take the form of emergency shutdown of the isolation system. Only the first possibility will be considered.

Failure in any part of the feedback circuit either would render the system inoperative automatically or would result in violent motion of the active element. The latter might occur because of the introduction of stray transients in the circuit or failure of some part which resulted in an instability in the circuit. During testing of the hybrid vibration isolation system, such failure resulted in the breaking of the spring attachment. In such cases, the dashpot acted ultimately as a restraining member. It is suggested that the dashpot be constructed to act as a clamp to restrain the suspended load in the case of spring failure. Actuation of the clamp would be accompanied by shutdown of the control valve electronics to prevent further motion of the active element.

Other modes of failure are possible. If the hydraulic power supply failed, emergency shutdown of the valve would render the active element both stiff and inoperative. If leaks developed in the plumbing between the valve and cylinder so that the active element became soft, some form of clamping arrangement could be employed. The clamp which would seize the rod and prevent further motion could be activated by a drop of static pressure within the cylinder.

CONCLUSIONS AND RECOMMENDATIONS

It is concluded that:

1. An active element can be made to act like any arbitrary impedance when a suitable sensor and feedback are employed. For example, it can look like a dashpot of arbitrary resistance or variable mass.

2. The introduction of an active element in an otherwise passive system can completely change the characteristics of the passive system. The resonance of the passive system can be suppressed.

3. The hybrid vibration isolation system provides isolation which is essentially independent of the load.

4. The hybrid vibration isolation system is capable of presenting a fairly stiff system with abrupt roll-off of stiffness, resulting in isolation greater than can be achieved with a comparable passive system.

5. Nonlinearities in the hydraulic system apparently may be a help or a hindrance and thus need to be better understood.

6. Some low-frequency amplification of response persists with the hybrid vibration isolation system, and improved means need to be developed which will allow shutdown of the active element at low frequencies.

It is recommended that:

1. Experimentation be continued with the basic apparatus to investigate other sensor and feedback arrangements.

2. The possible advantages and disadvantages of nonlinearities be investigated.

3. A more sophisticated prototype be constructed and tested. Emphasis should be placed on weight reduction.

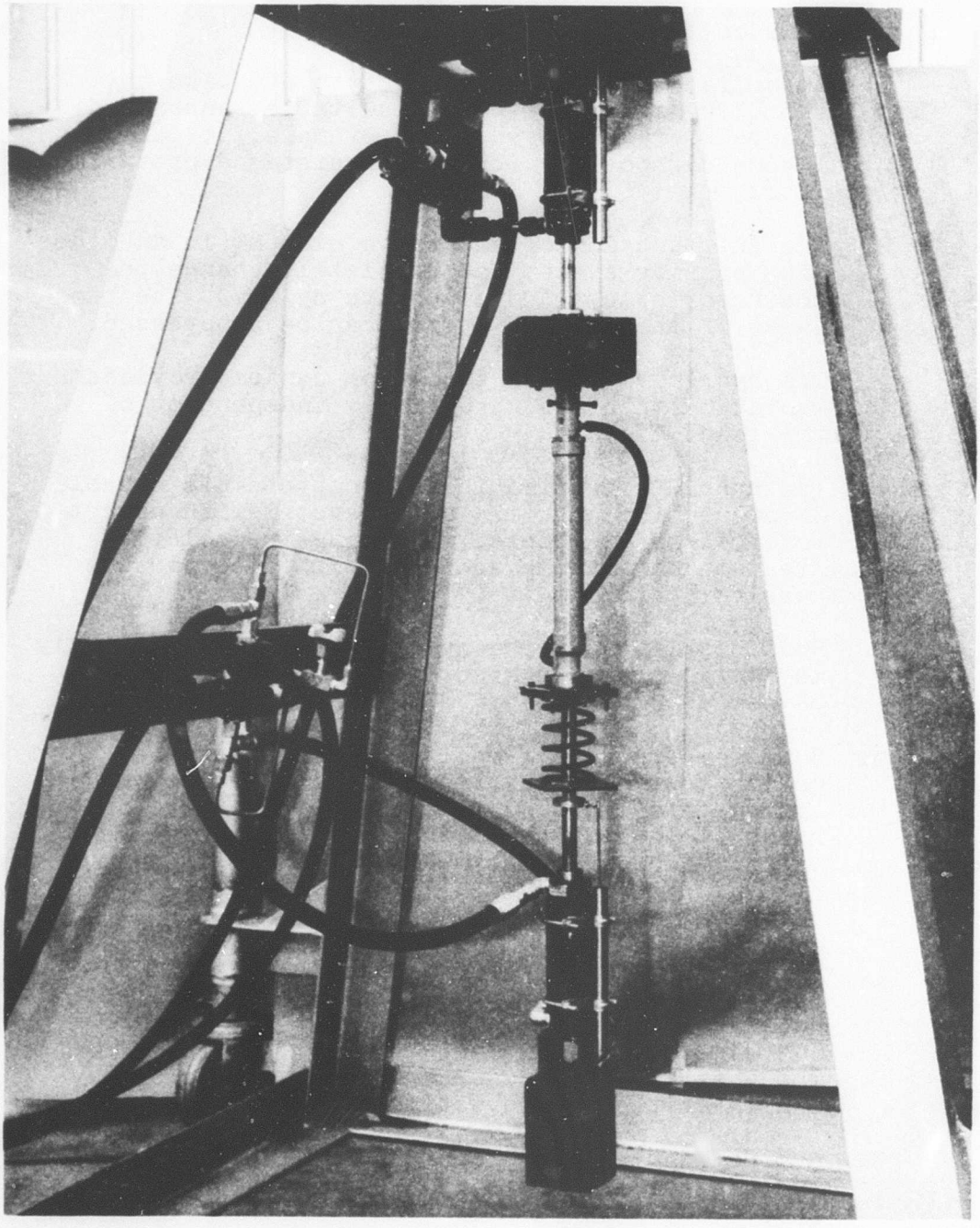

Figure 1a. Hybrid Vibration Isolation Model Mounted for Testing.

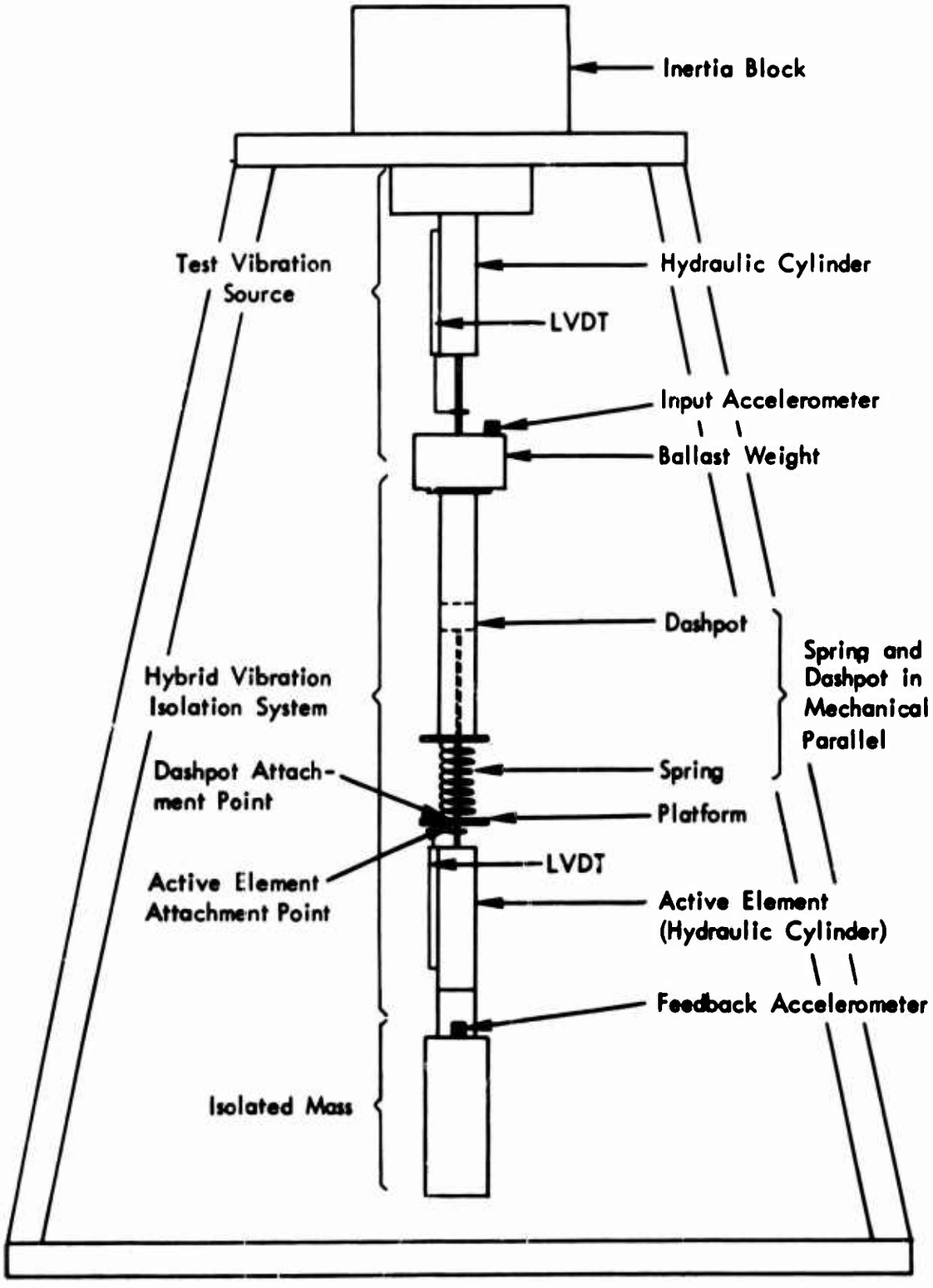

Figure 1b. Detail of Hybrid Vibration Isolation Model.

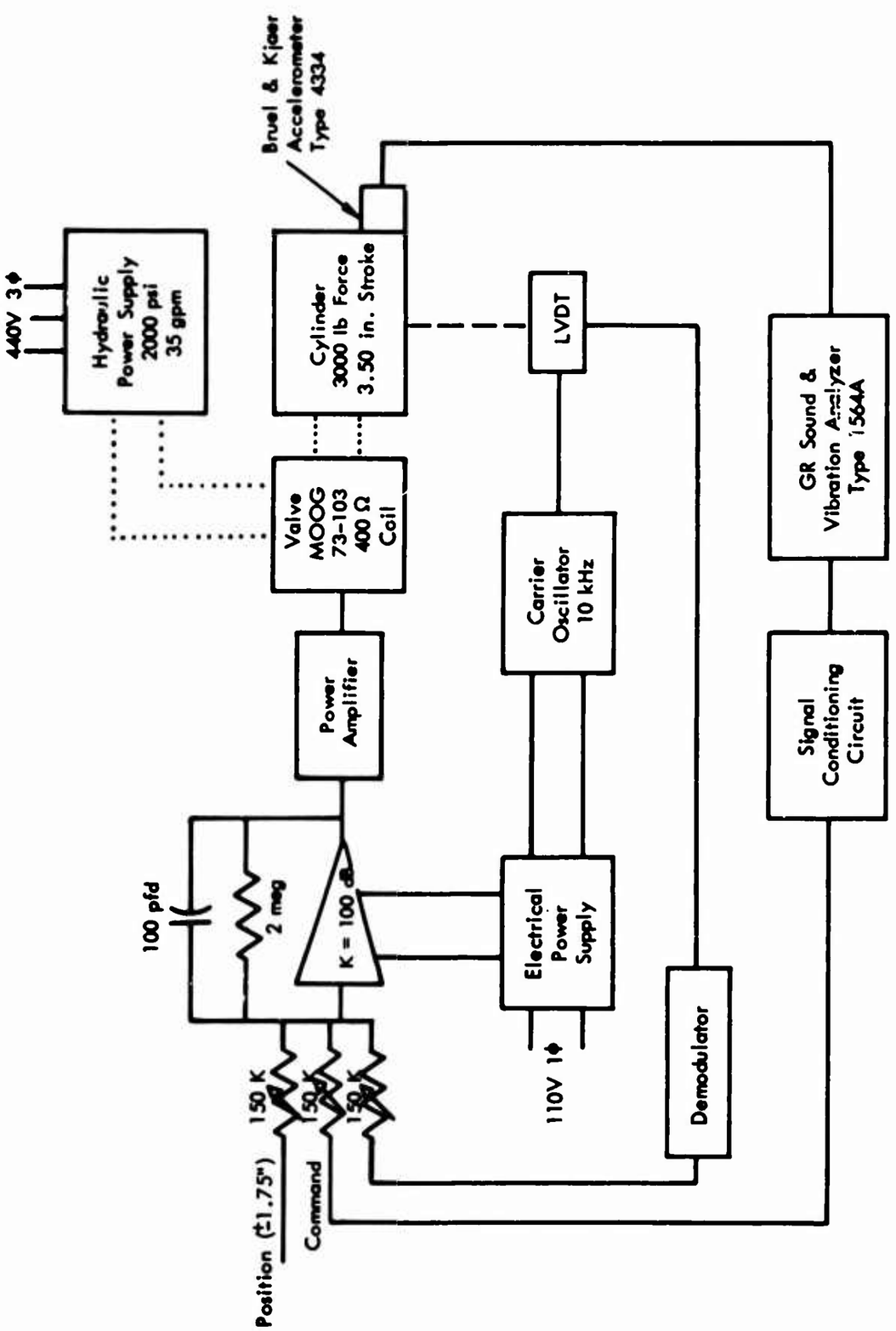

Figure 2. Block Diagram for Hybrid Vibration Isolation System.

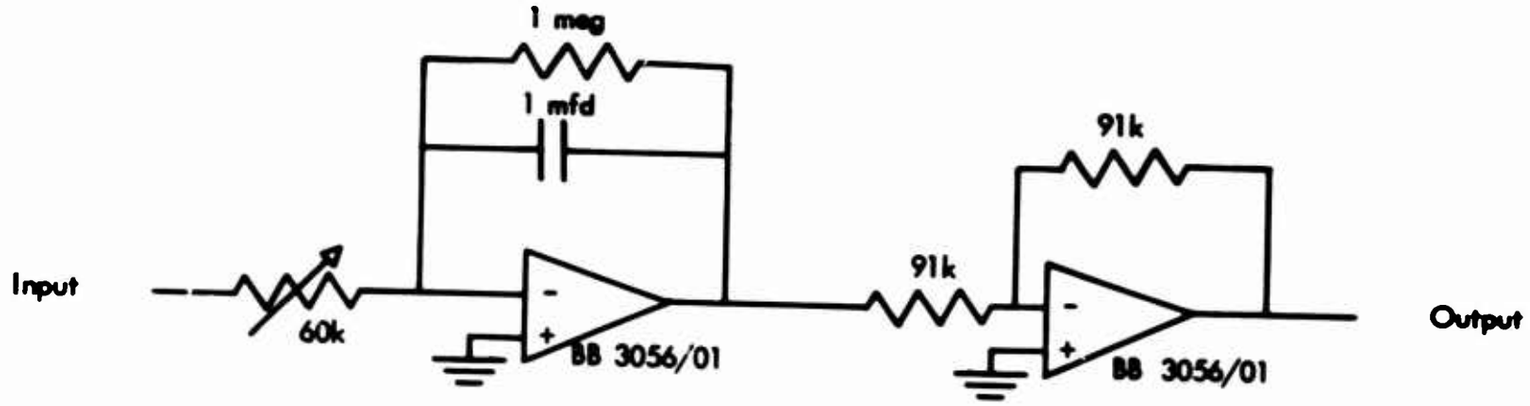

Figure 3. Signal Conditioning Circuit.

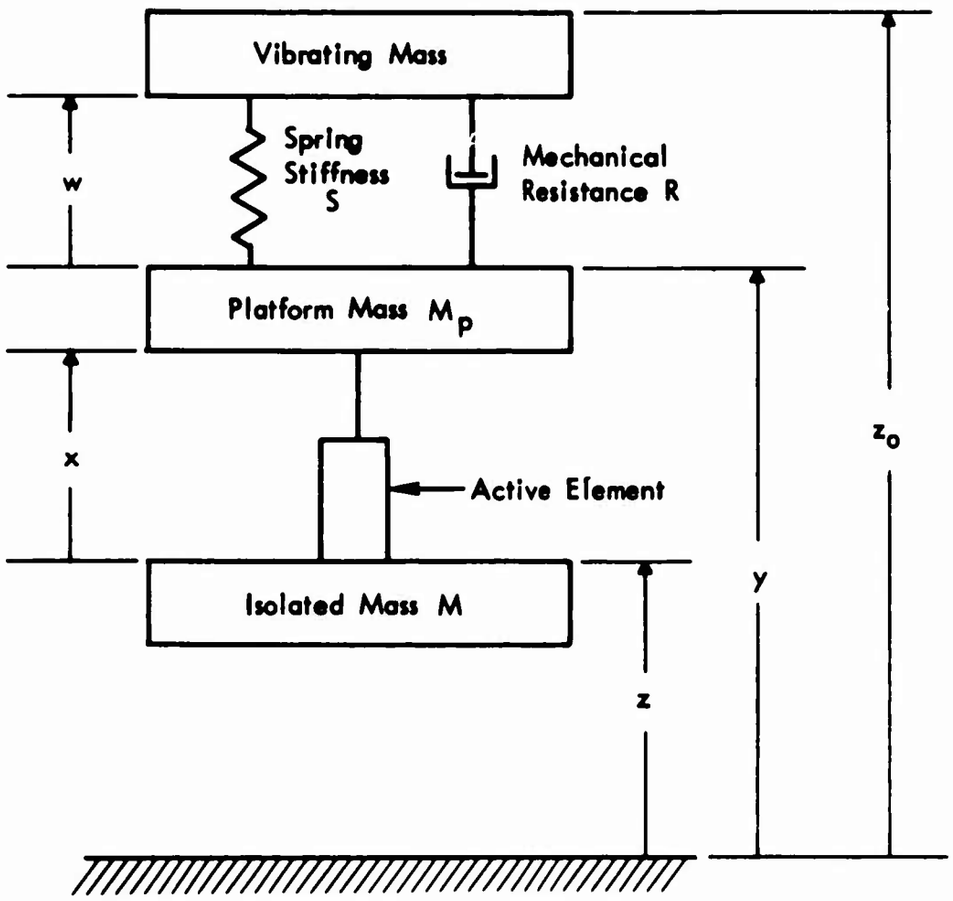

Figure 4. Schematic Representation of the Hybrid Vibration Isolation System Showing the Displacements and the Sense of Their Direction as Used in the Text.

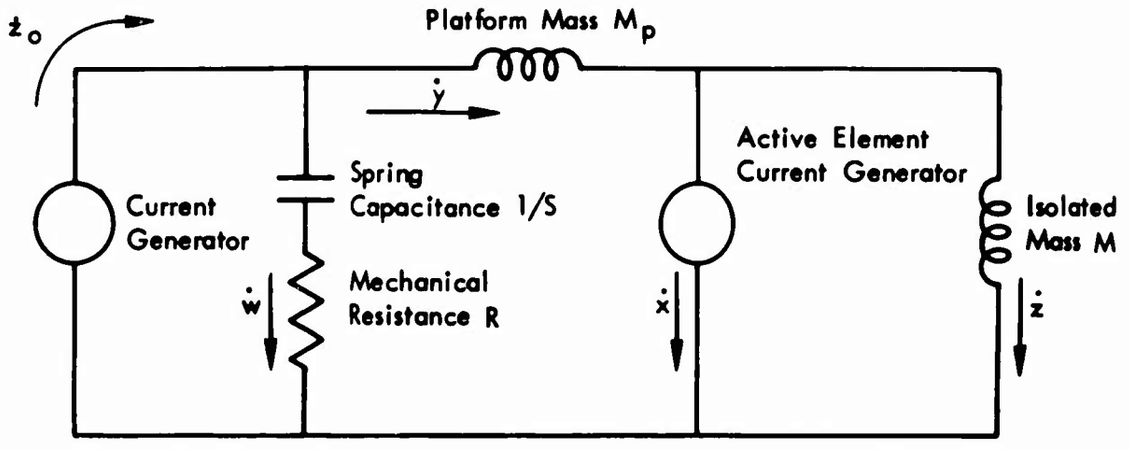

Figure 5. Equivalent Electrical Circuit Using Voltage-Force, Current-Velocity Analogy for the Hybrid Vibration Isolation System.

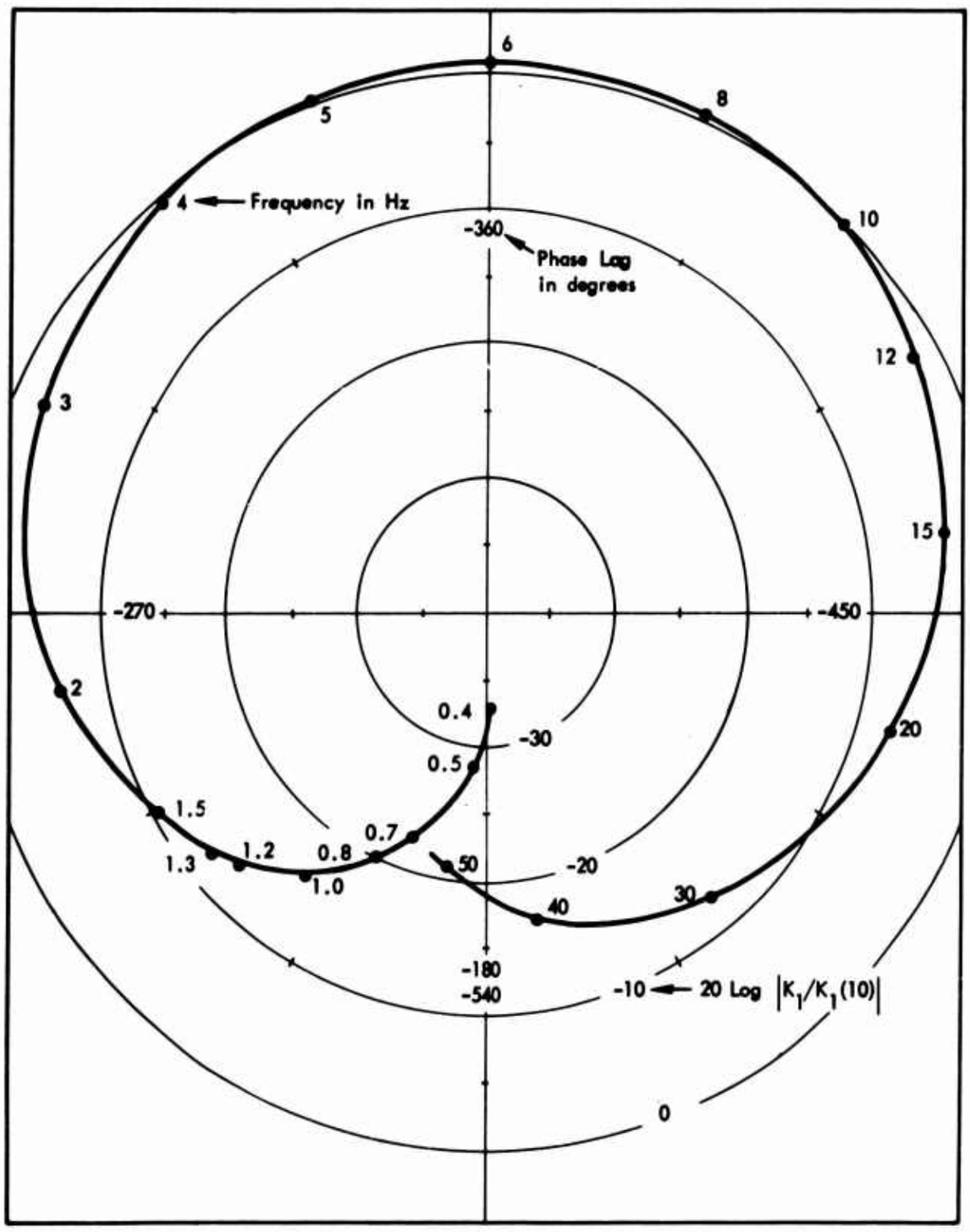

Figure 6. Polar Plot of K_1 Where $K_1 = x/z$.

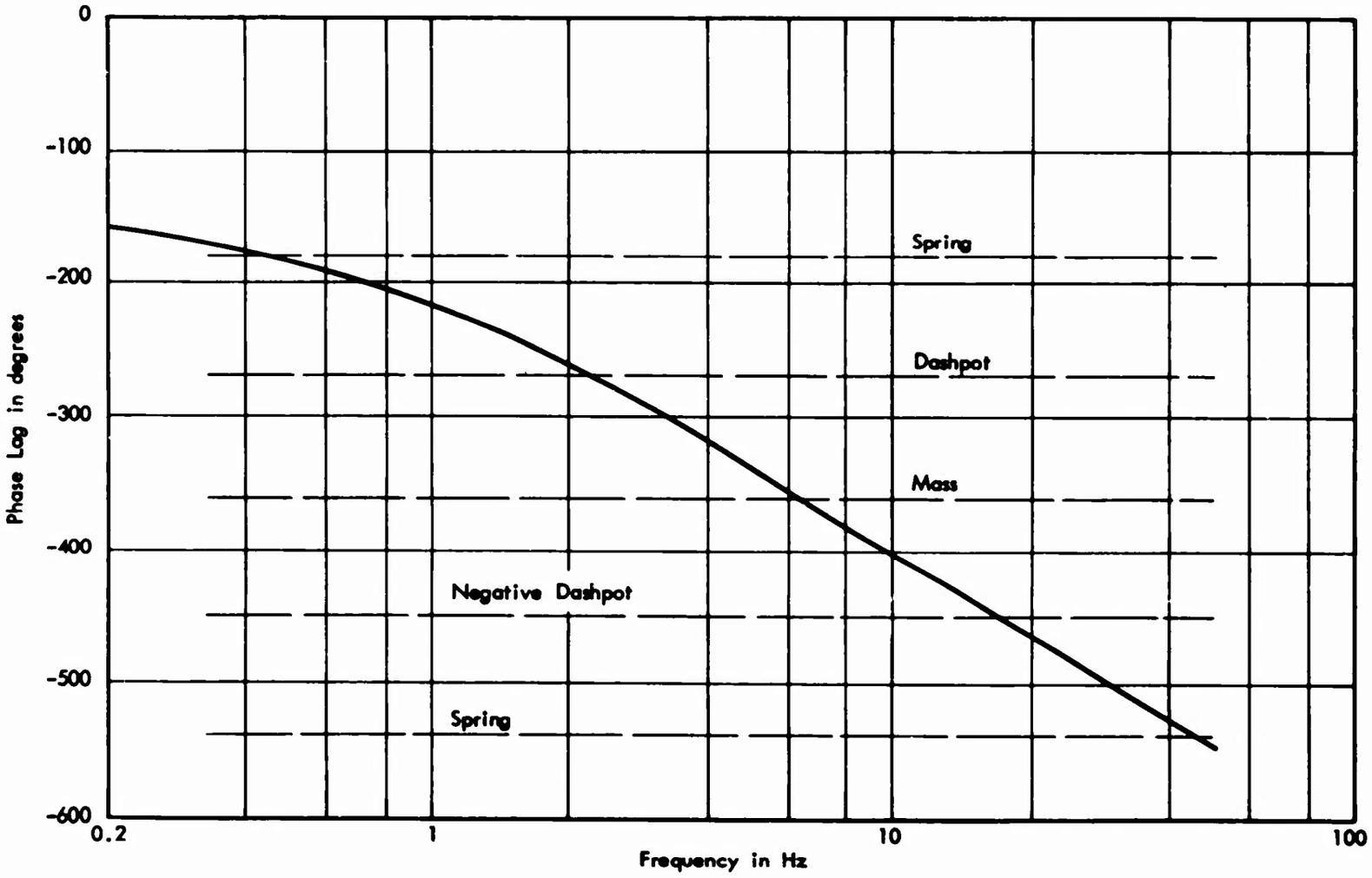

Figure 7. Comparison of Active Element Displacement Phase Relative to Isolated Mass Displacement with Equivalent Passive Elements.

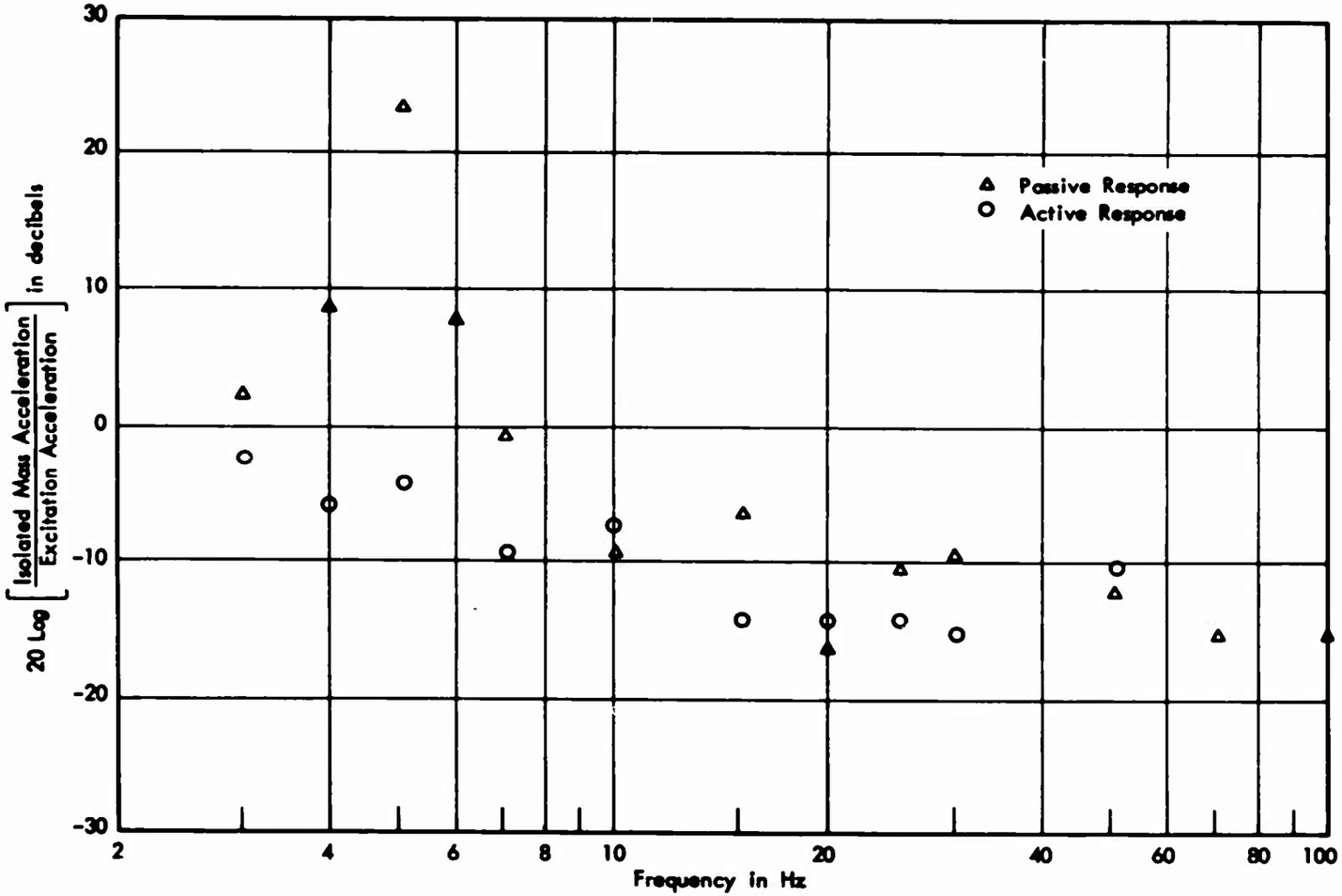

Figure 8. Comparison of Vibration Isolation with Active and Passive Response of the Hybrid Vibration Isolation System for Low-Level Excitation. Excitation Acceleration Levels Generally Ranged Between 10 and 20 Decibels Below 1 g rms. The Suspended Mass was 20 Pounds.

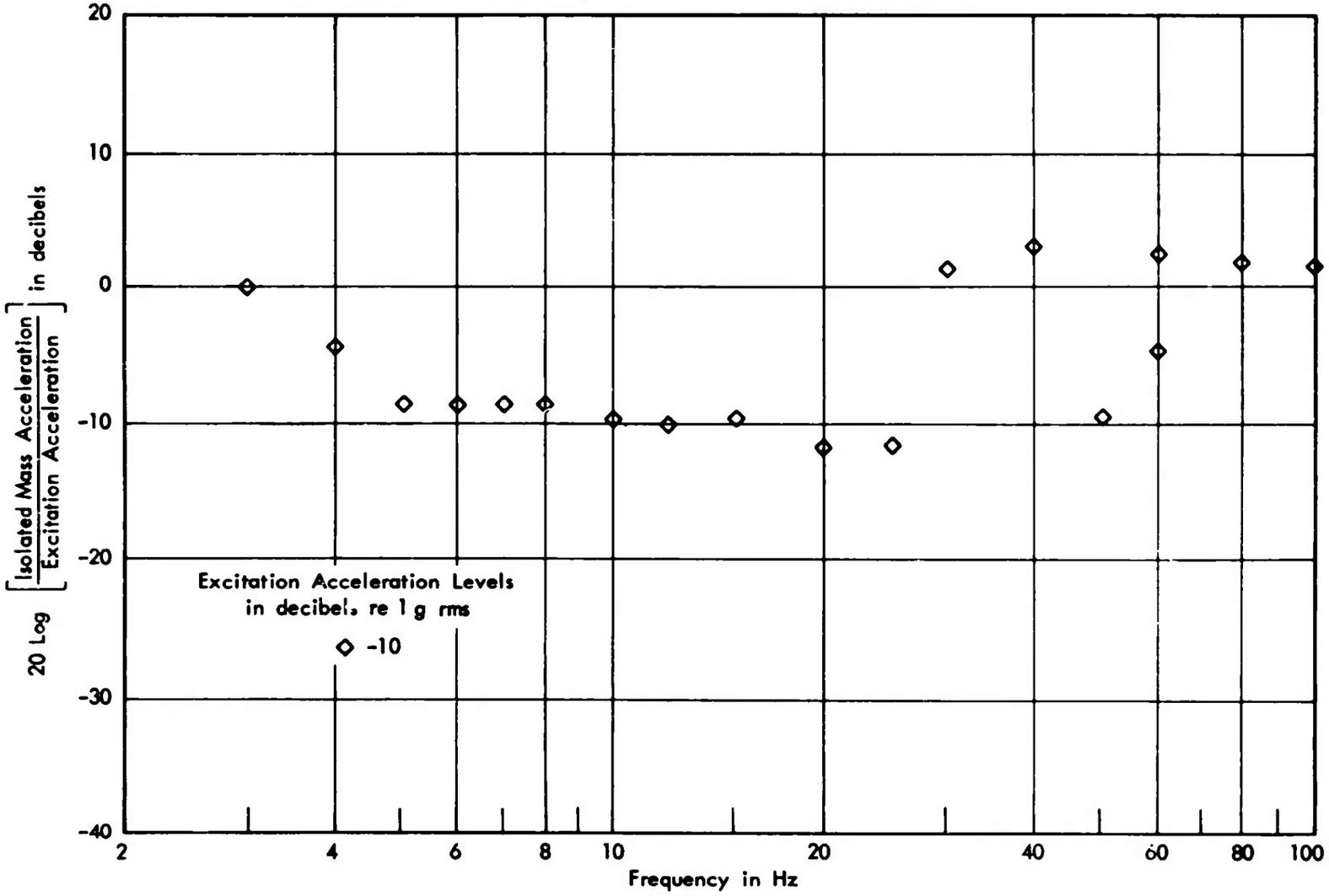

Figure 9. Vibration Isolation Observed with No Suspended Mass.

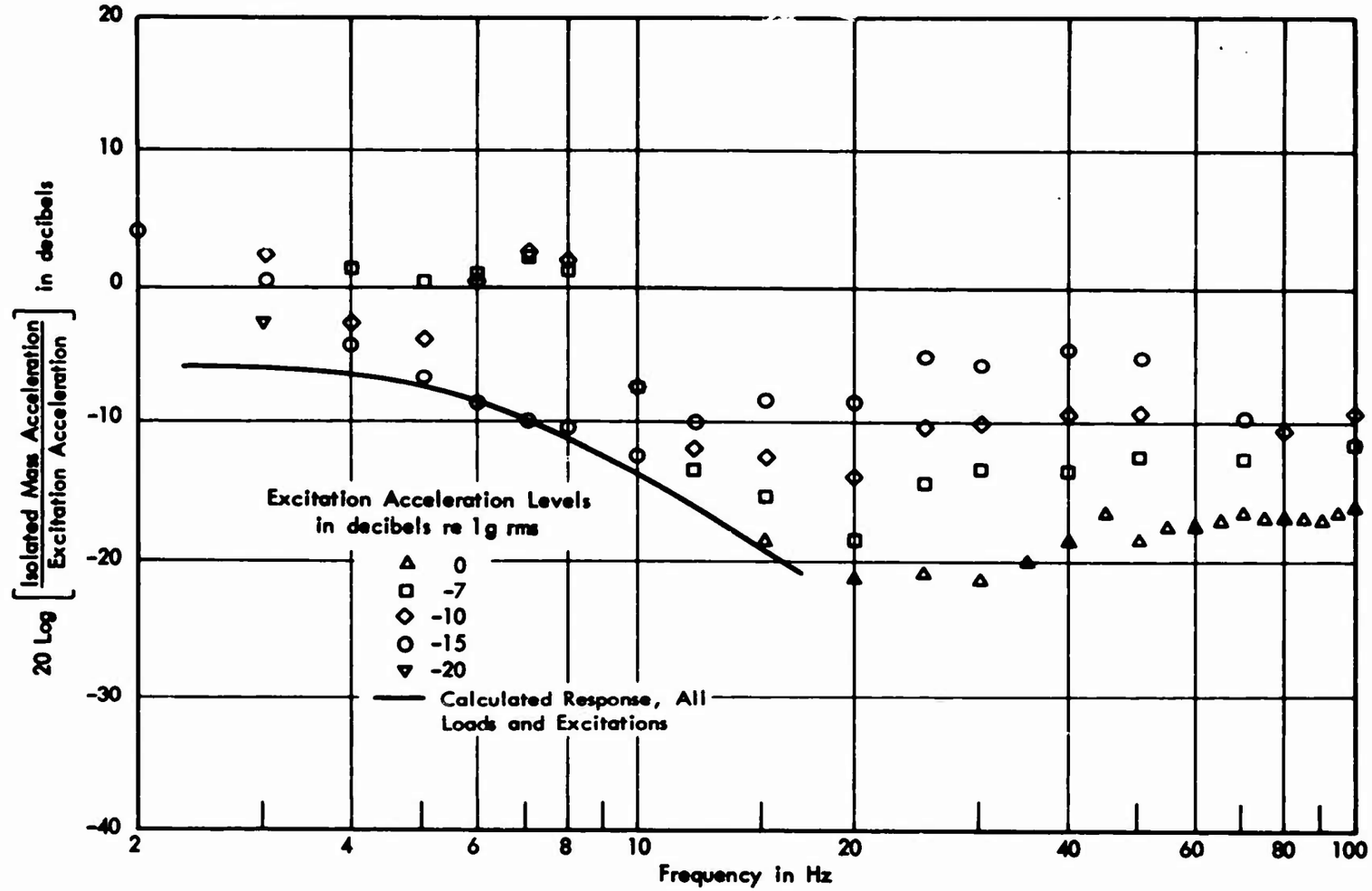

Figure 10. Vibration Isolation Observed with a 20-Pound Suspended Mass for Various Levels of Excitation Acceleration Compared with Calculated Response.

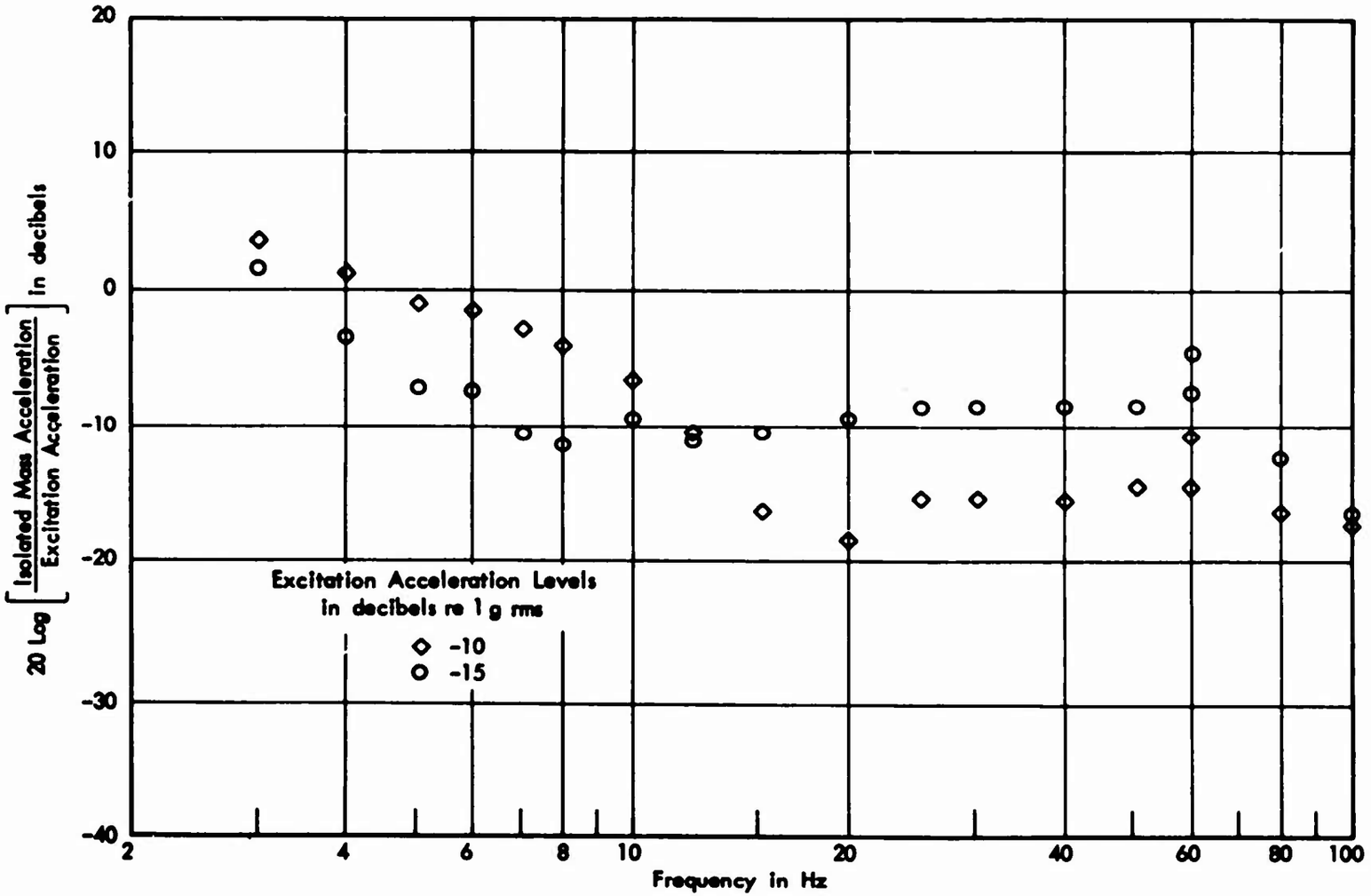

Figure 11. Vibration Isolation Observed with a 40-Pound Mass for Various Levels of Excitation Acceleration.

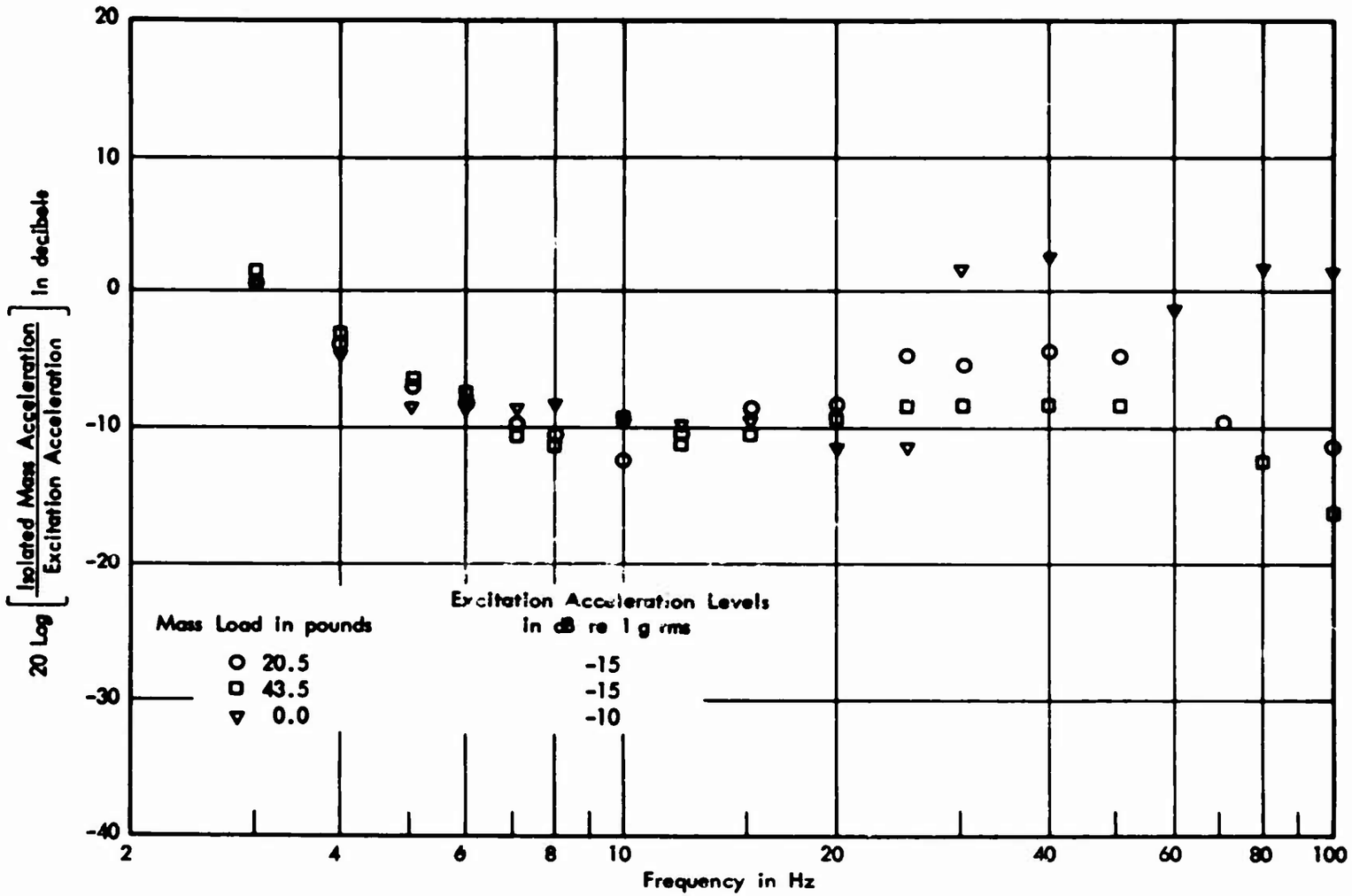

Figure 12. Vibration Isolation Observed with the Hybrid Vibration Isolation System for Several Mass Loads.

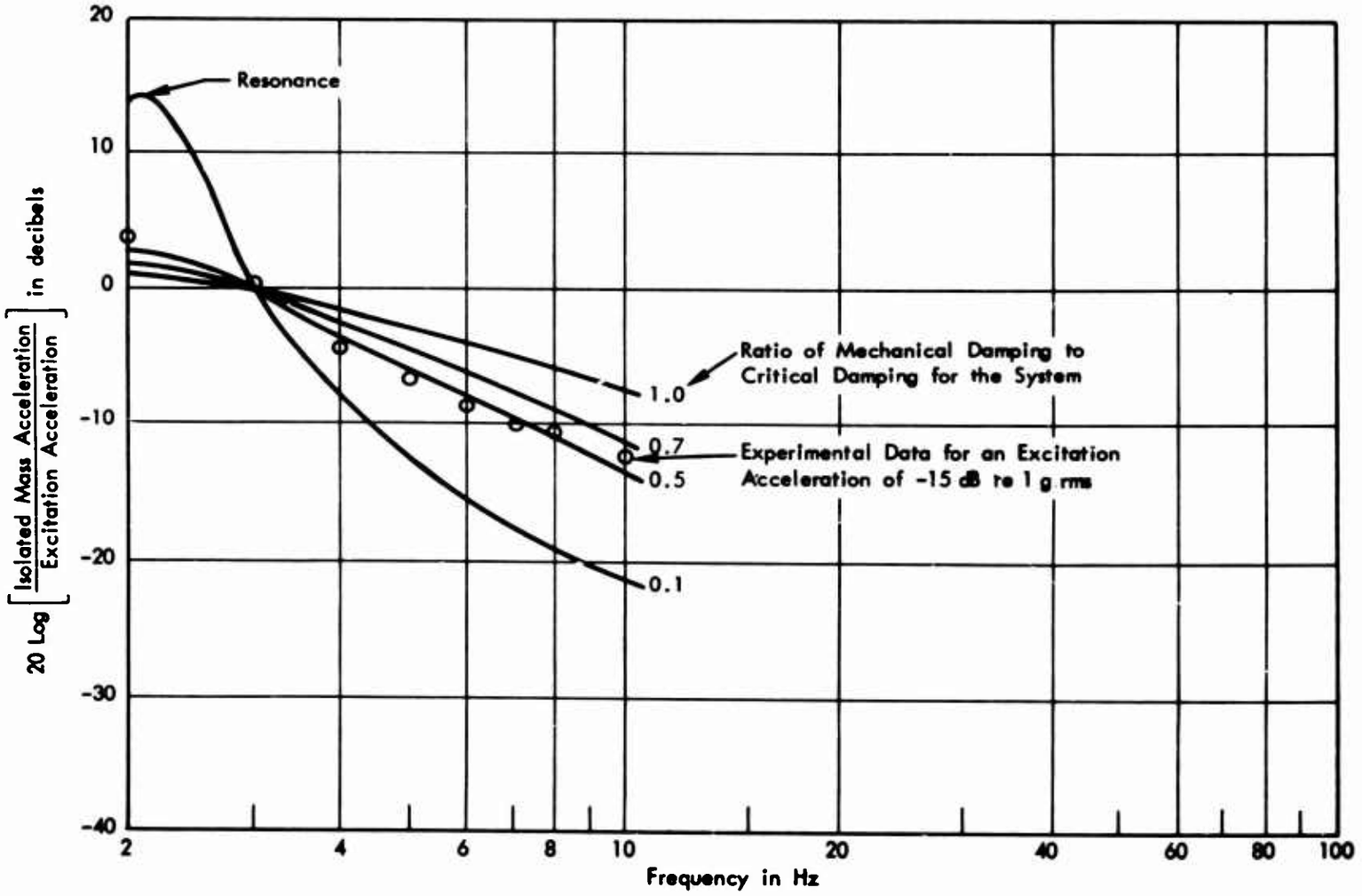

Figure 13. Hybrid System Vibration Isolation Observed on a Suspended 20-Pound Mass Compared with Calculated Isolation with a Passive Isolation System.

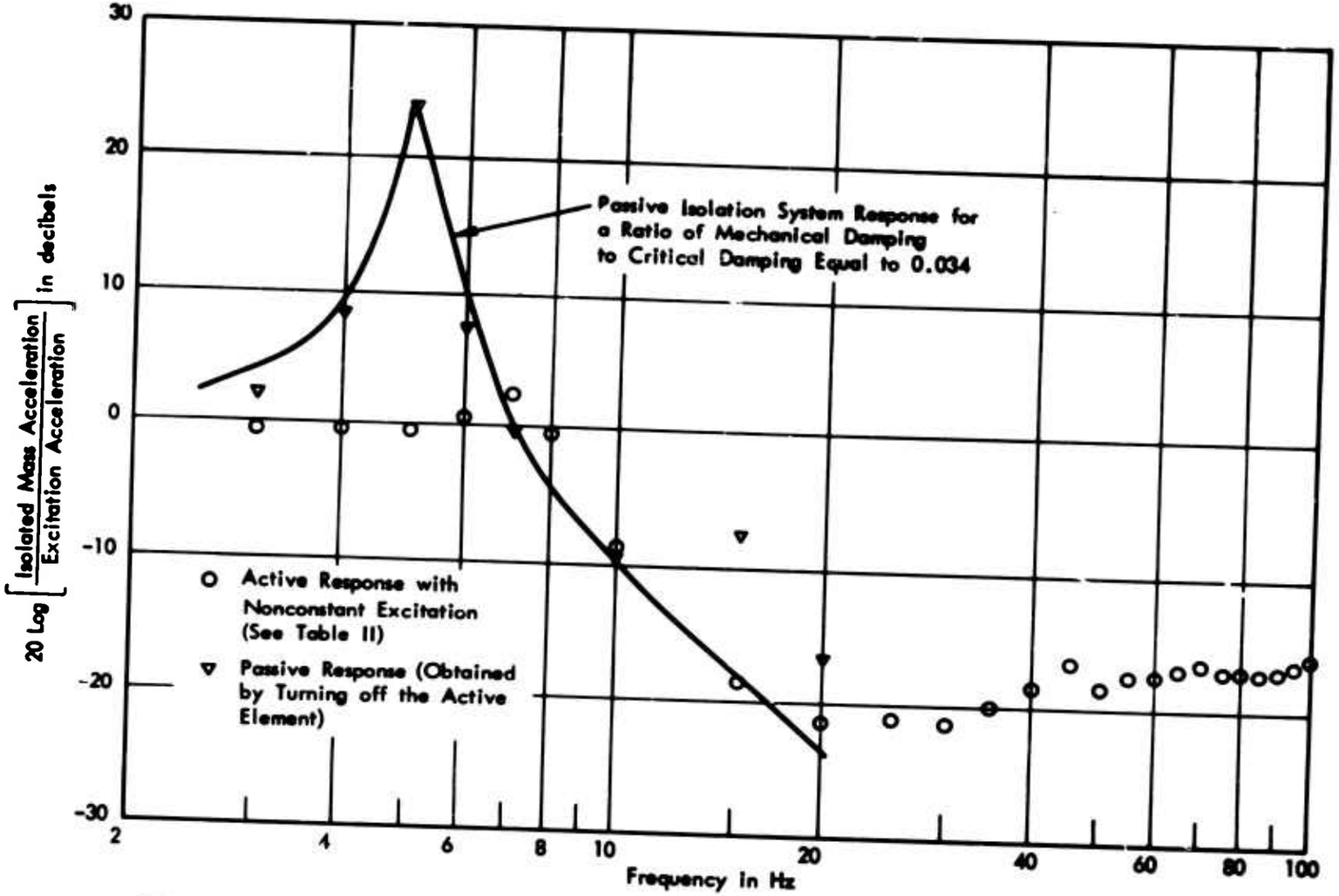

Figure 1'. Vibration Isolation Observed on a Suspended 20-Pound Mass Compared with Measured and Calculated Isolation with a Passive Isolation System.

APPENDIX
ANALYSIS OF THE HYBRID VIBRATION ISOLATION SYSTEM

Reference should be made to either Figure 4 or Figure 5 for the following discussion. In terms of the electrical analog shown in Figure 5, the current flow at junctions gives the following relationships:

$$\dot{z}_o = \dot{y} + \dot{w} \tag{20}$$

and

$$\dot{y} = \dot{x} + \dot{z} \quad . \tag{21}$$

Voltage around the closed loop gives

$$\dot{w}\, R + S \int \dot{w}\, dt = M_p\, \ddot{y} + M\ddot{z} \quad . \tag{22}$$

Substitution of Equations 20 and 21 into Equation 22 gives

$$(\dot{z}_o - \dot{x} - \dot{z})\, R + S \int (\dot{z}_o - \dot{x} - \dot{z})\, dt =$$

$$= M_p(\ddot{x} + \ddot{z}) + M(\ddot{z}) \quad . \tag{23}$$

Define a proportionality constant K such that

$$\dot{x} = K\dot{y} \tag{24}$$

The quantity K is defined such that when K is unity, $\dot{z}$ is zero; complete vibration isolation is achieved.

Define a second quantity K_1 such that

$$1 + K_1 = (1 - K)^{-1} \quad ; \tag{25}$$

then

$$\dot{x} = K_1\dot{z} \quad , \tag{26}$$

which follows from the relationship between the variables x, y, and z shown in Figure 4.

Substitute Equation 26 into Equation 23 to obtain

$$m\ddot{z} + R_m\dot{z} + S_m z = R\dot{z}_o + Sz_o \tag{27}$$

where

$$\left.\begin{aligned} m &= M + M_p(1 + K_1) \quad , \\ R_m &= R(1 + K_1) \quad , \\ \text{and} \quad S_m &= S(1 + K_1) \quad . \end{aligned}\right\} \tag{28}$$

Steady-state response to sinusoidal excitation is obtained from Equation 27 by assuming that the time dependence of z_o is of the form exp ($i\omega t$). The resulting expression for steady-state response is

$$z = \frac{(i\omega R + S)\, z_o}{-m\omega^2 + iR_m\omega + S_m} \quad . \tag{29}$$

The quantity K_1 is complex, so that the response function $|z/z_o|$ which is obtained from Equation 29 takes the form

$$\left|\frac{z}{z_o}\right| = \frac{(\omega R)^2 + S^2}{\sqrt{X^2 + Y^2}} \tag{30}$$

where

$$\left.\begin{aligned} X &= -[M + M_p \mathrm{Re}(1 + K_1)]\omega^2 - R\omega \mathrm{Im}(K_1) + S\,\mathrm{Re}(1 + K_1) \\ \text{and } Y &= -M_p \mathrm{Im}\,(K_1)\omega^2 + R\,\mathrm{Re}(1 + K_1)\omega + S\,\mathrm{Im}(K_1) \quad . \end{aligned}\right\} \tag{31}$$

The transient response is obtained by setting z_o equal to zero in Equation 27 and assuming that z is of the form exp (γt). The resulting expression for the transient solution is

$$z = z' e^{\gamma t} \tag{32}$$

where z' is the initial displacement and γ is a complex quantity given by

$$\gamma = \frac{-R_m \pm \sqrt{R_m^2 - 4m\, S_m}}{2m} \quad . \tag{33}$$

In general, γ will have a real and an imaginary part. For stability, the real part must be negative. The solutions for the real and imaginary parts are quite complicated and as a consequence are not very useful and are not presented here. However, for the special case that

$$M_p \left| 1 + K_1 \right| \gg M \quad , \tag{34}$$

Equation 33 takes on a relatively simple form. In the case that Equation 34 holds,

$$\gamma = -\alpha \pm i\beta \tag{35}$$

where $\alpha = R/2\ M_p$

and $\beta = \sqrt{\frac{S}{M_p} - \frac{R^2}{4M_p^2}}$. (36)

Values for the various components which were used for calculating response in the text are given in Table V. As a matter of interest, the spring was designed for a surge frequency of 120 Hz, which is well above the frequency range of interest.

TABLE V. COMPONENT VALUES USED FOR CALCULATING RESPONSE	
Component	Value and Units
Isolated Mass M*	
Active element assembly, effective weight hoses, box mounting fixture, and accelerometers	0.44 slug
Nominal 20-pound load	0.64 slug
Nominal 40-pound load	1.35 slugs
Platform Mass M_p	
Active element rod, dashpot rod, attachment plate, and third of spring mass	0.13 slug
Spring Stiffness S	1080 lb force/ft
Dashpot Resistance R	2.38 lb force sec/ft
Value of K_1 at 6 Hz where K_1 is real	3.48 (dimensionless)

* For no load, the isolated mass was 0.44 slug, while for a nominal 20-pound load or a nominal 40-pound load, it was 1.08 slugs or 1.79 slugs, respectively.

Unclassified

Security Classification

DOCUMENT CONTROL DATA - R & D

(Security classification of title, body of abstract and indexing annotation must be entered when the overall report is classified)

1. ORIGINATING ACTIVITY (Corporate author)
Bolt Beranek and Newman Inc.
Van Nuys, California

2a. REPORT SECURITY CLASSIFICATION
Unclassified

2b. GROUP

3. REPORT TITLE
FEASIBILITY STUDY OF A HYBRID VIBRATION ISOLATION SYSTEM

4. DESCRIPTIVE NOTES (Type of report and inclusive dates)
Final Report

5. AUTHOR(S) (First name, middle initial, last name)
David A. Bies

6. REPORT DATE
August 1968

7a. TOTAL NO. OF PAGES
42

7b. NO. OF REFS

8a. CONTRACT OR GRANT NO.
Contract DAAJ02-67-C-0082

b. PROJECT NO.
Task 1F125901A14608

c.

d.

9a. ORIGINATOR'S REPORT NUMBER(S)
USAAVLABS Technical Report 68-54

9b. OTHER REPORT NO(S) (Any other numbers that may be assigned this report)
BBN Report 1620

10. DISTRIBUTION STATEMENT
This document has been approved for public release and sale; its distribution is unlimited.

11. SUPPLEMENTARY NOTES

12. SPONSORING MILITARY ACTIVITY
U. S. Army Aviation Materiel Laboratories
Fort Eustis, Virginia

13. ABSTRACT

The fluctuating lift of a helicopter rotor gives rise to undesirable vibration over a broad frequency range which in some cases may extend to as low as 3 Hz. Vibration isolation over this frequency range is very difficult to achieve with either a purely passive or an active vibration isolation system. A passive system will work well at high frequencies, but it will always have a low-frequency resonance where excitation will be amplified rather than reduced. An active system may work well at low frequencies, but it will have trouble meeting the frequency response requirements at high frequencies. This investigation of the feasibility of combining an active and a passive system has been conducted to gain the advantages of both. The report shows that an active system may be used to control the resonant response of a passive system while preserving the isolation achieved at high frequencies. Isolation over a broad frequency range may be obtained by this means with only a small amplification of response at low frequencies.

DD FORM 1 NOV 68 1473 REPLACES DD FORM 1473, 1 JAN 64, WHICH IS OBSOLETE FOR ARMY USE.

Unclassified

Security Classification

14. KEY WORDS	LINK A		LINK B		LINK C	
	ROLE	WT	ROLE	WT	ROLE	WT
vibration isolation helicopter vibration isolation active vibration isolation active shock isolation						